ELSEVIER

Chemical Engineering Journal 128 (2007) 105–114

Chemical Engineering Journal

www.elsevier.com/locate/cej

The dynamics and structure of a liquid–solid fluidized bed in inclined pipes

Bachtiyar Yakubov [a], Josef Tanny [a,b,*], David Moalem Maron [a], Neima Brauner [c]

[a] *Holon Institute of Technology, P.O.B. 305, Holon 58102, Israel*
[b] *Agricultural Research Organization, POB 6, Bet Dagan 50250, Israel*
[c] *Faculty of Engineering, Tel Aviv University, Tel Aviv 69978, Israel*

Received 17 July 2006; received in revised form 12 October 2006; accepted 18 October 2006

Abstract

The dynamics and structure of a fluidized bed in inclined columns are investigated experimentally. Experiments were conducted in two glass columns of $L/D = 95$ and 150, and diameters of 2.58 and 2.78 cm, which can be positioned in the whole range of inclination angles, from horizontal to vertical. The fluidizing agent is water and the grain material is particles of different densities and characteristic diameters. Measurements of the pressure loss, flow rate of the fluidizing agent and fluidized bed position and height are carried out. Particle flow patterns were visualized using a digital camera. The expansion process of the fluidized bed depends strongly on the inclination angle. Consequently the critical velocity for the bed escape varies with the column inclination angle and exhibits a maximum at about 45°. The column length was found to have a minor effect on the phenomena involved.

Keywords: Escape critical flow rate; Particle density; Particle diameter; Initial bed height; Pressure loss; Inclination angle

1. Introduction

Many important processes occur under conditions of fluidization in vertical or inclined ducts. Such processes include refining from the sulfur and hydro-cracking of oil fractions, hydrogenization of coal for production of fuel oil, refining of sewage, processes of oil-extraction, washing the grains in a sand cork formed during oil production processes [1] and cooling systems of nuclear power plants.

Previous investigations of a fluidized bed in vertical ducts are reported in [1–5]. These works were mainly focused on two-phase, solid-air flows in large duct diameters. Literature survey indicates that in spite of its practical importance, very few studies have been reported on fluidized bed in inclined pipes. These flows are important, for example, for oil drilling and pumping processes. In recent years more and more oil fields utilize inclined wells. This is mostly used in marine oil fields, where several inclined wells are drilled from a single platform towards different directions.

O'dea et al. [6] studied beds inclined at angles between 45° and 90° to the horizontal using four different types of powders and air as the fluidizing medium. Flow regimes and transition condition have been identified experimentally and verified by a theoretical model. Hudson et al. [7] who studied liquid–solid beds, investigated small inclinations of only up to 10° from the vertical. They measured local holdup and circulation pattern of the liquid and solid phases, and developed a simple model that predicted the solid circulation pattern.

The hydro-transportation in horizontal and slightly inclined pipes was considered in [8,9] and pneumatic transportation was studied in [10]. Doron et al. [8] studied the effect of inclination on the characteristics of the bed formed in horizontal and slightly inclined tubes (up to 7°). They reported a considerable effect of the inclination on the flow characteristics, even for the relatively small angles considered in their study. Ercolani et al. [9] studied experimentally the solid bed formation mechanism during shutdown in the elbow of inclined slurry pipeline sections. Inclination elbow angles of up to 30°, with the same elbow curvature, were considered. In particular, they measured the solid bed profile and studied the effect of elbow position on this profile. Sarkar et al. [10] studied the flow of solid particles from a vertical fluidized bed to a receiving vessel through an inclined

* Corresponding author.
E-mail address: tanai@hit.ac.il (J. Tanny).

1385-8947/$ – see front matter © 2006 Elsevier B.V. All rights reserved.
doi:10.1016/j.cej.2006.10.020

Nomenclature

A	pipe cross section area
d_p	particle diameter
D	pipe diameter
H	fluidized bed height
H_0	initial bed height
L	pipe length
P	pressure
Q	fluidizing agent flow rate
Q_c	critical flow rate
U	velocity
Z	vertical coordinate

Greek symbols

α	pipe inclination angle
ε	holdup
ρ_p	particle density

downward pipe. They investigated the effects of the connecting pipe length, diameter, inclination angle and fluidizing agent velocity on the flow rate of solid particles from the fluidized bed to the receiving vessel. Hutter and Scheiwiller [11] carried out a numerical study of the downward granular flow in an inclined channel. They obtained the particle velocity profile assuming a smooth boundary condition at the channel wall. Masliyah et al. [12] studied the enhancement of separation of light and heavy particles from suspensions using inclined channels. They observed that at a fixed set of operating conditions, the increase of the off-vertical inclination results in a greater degree of separation. A relatively short channel of 0.4 m long was used, thereby limiting the study to the stage of fluid filtration through the particles.

The results of the above studies indicate a considerable effect of tube inclination angle on fluid–particle interactions and the resulting flow characteristics. In many practical applications and industrial processes, the use of a fluidized bed in inclined pipes is considered, owing to the belief that inclined pipes tend to give higher solid circulation rate in the bed and less instability problems [13]. It is noted that in this work the term "fluidized bed" refers to vertical, inclined or horizontal two-phase flow, in which particles are not transported away with the liquid, but kept within the system. For example, such systems may be realized in oil exploitation processes. This is a somewhat more general definition than the usual one, which refers to systems where a maximal contact area between particles and liquid is required (e.g. vertical fluidized beds in reactors, etc.).

This paper presents the results of an experimental investigation of the fluidization processes and the onset of hydro-transport of solid particles in upward inclined pipes. The study had two major goals: the first is to investigate experimentally the effect of the pipe inclination angle and the flow rate of the fluidizing agent on the structure and stability of the fluidized bed, and on the associated flow characteristics in upward inclined pipes. The second is to study the effect of particle density, diameter and initial bed height on the above processes.

2. Experimental setup and procedures

2.1. The apparatus

A schematic description of the experimental setup is shown in Fig. 1. Experiments were conducted in two different setups: one with a relatively short column of $L = 240$ cm (hereafter referred to as short pipe facility—SPF), and the other with a longer one of $L = 420$ cm (hereafter referred to as long pipe facility—LPF). Both columns were glass pipes of diameters $D = 2.58$ (SPF) and

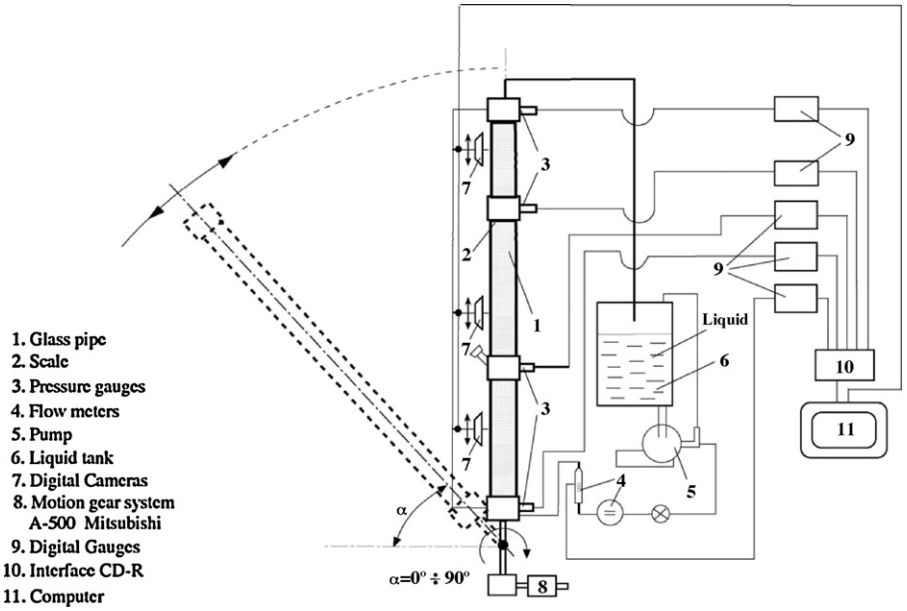

Fig. 1. A schematic description of the experimental apparatus with the long pipe.

$D = 2.78$ cm (LPF). In the following, the numbers in parentheses indicate the item number in Fig. 1 (illustrating the LPF). The transparent glass pipe (1) allowed the visualization and recording of the flow and transport processes during the experiment. The pipe could be positioned at inclination angles in the whole range from horizontal to vertical, i.e., $\alpha = 0$–90°. Thus vertical, horizontal and inclined fluidized beds could be studied. The position of the pipe was set by a motorized system (8). The pipe was equipped with inner circular nets, embedded at its top exit and bottom inlet, to prevent the escape of particles from the pipe. A scale (2) was attached along the pipe to facilitate the measurements of the instantaneous fluidized bed position and height. The accuracy of this measurement was estimated as ±0.5 cm. A water tank (6) and a pump (5) were used to circulate the working fluid (water) through the pipe. This facility also allows experiments on air–water (three-phase) fluidized bed processes (not reported here).

Four electronic pressure transducers (3) (manufactured by STS, Sirnach, Switzerland) were installed to measure the pressure at four locations along the pipe at distances of 0 (P_1), 105 (P_2), 265 (P_3) and 420 (P_4) cm from the pipe inlet. The respective measurement ranges of the pressure transducers were 0–1000, 0–600, 0–600 and 0–250 mbar. The error in the pressure measurements was estimated as ±1 mbar. The output of the pressure transducers was monitored by digital gauges (9) and was recorded by an interface (10) to a PC (11).

The flow rate was measured by two flow meters (4). One flow meter was an electronic rotameter (manufactured by Kobold, Germany) with a range of 0–12 l/min and an error of ±0.015 l/min. In the SPF, a rotameter (ROTA) was used with a measurement range of 0–10.5 l/min and an error of ±0.015 l/min. The second flow meter was a commercial cumulative meter (METERS) with an error of ±0.1 l/min. In the LPF, three digital cameras (7) connected to a PC recorded the particle flow patterns and the structure and height of the fluidized bed at different positions along the pipe. To improve the output of the cameras, the pipe was illuminated by a white light source in both facilities.

Both columns allowed the investigation of the fluidization process of the grain material by one-phase medium (liquid). In all the experiments reported in this study, the working fluid was water. In most of the experiments, the grain material was small particles of silica gel, with a characteristic diameter of 3.2 mm, and a density of 1.25 g/cm^3. Experiments were also carried out to study the effect of particle diameter, concentration and density on the fluidization process. For that purpose, particles of the same density (1.25 g/cm^3) and three different diameters, 1.5, 2.5 and 3.2 mm, were used. The effect of the density was investigated by using two types of particles of nearly the same diameter, 1.2–1.4 and 1.5 mm, and densities of 2.65 and 1.25 g/cm^3, respectively.

Several types of experiments were carried out in this study, most of them conducted in both columns (SPF and LPF). The critical flow rate for the bed escape as a function of inclination angle was investigated under various operating conditions: different average concentration of particles in the pipe, different particle density and diameter and different time periods of operation at a given flow rate (the latter was studied only in the LPF). The time period effect was examined since at certain inclination angles, operating the system over long time periods (from 10 up to 120 min) at a given flow rate, caused a slight reduction in the escape flow rate as compared to a relatively short-term operation. This issue will be further discussed below in the results.

Table 1
Summary of the experimental conditions

Parameter (units)	Values or range of values
Columns diameter (cm)	2.58, 2.78
Columns length (m)	2.4, 4.2
Particle diameter (mm)	1.5, 2.5, 3.2
Particle density (g cm^{-3})	1.25, 2.65
Flow rate (l/min)	0–12
Initial bed height (m)	0.025, 0.125,0.25, 0.35, 0.45, 0.6
Inclination angle (°)	0 (horizontal)–90 (vertical)

2.2. Experimental procedures

To start an experiment, a certain amount of particles was introduced into the pipe, at a vertical position. The concentration (amount) of particles is designated as the initial height of particles in the vertical pipe without flow. Then, the pipe was positioned at the prescribed inclination. To study the effect of the concentration of particles on the fluidization process, experiments were carried out with six different amounts of particles in the pipe, corresponding to H_0, the initial height of the particles measured from the pipe bottom when the pipe is at a vertical position.

The physical conditions of the experimental study are summarized in Table 1.

Each experiment began at a low flow rate of the fluidizing liquid (water). This flow rate was then increased to a higher value in order to follow the evolution of the fluidized bed and the pressure drop as a function of the water flow rate. After each adjustment of the flow rate the system was allowed to operate between 0.5 and 1.5 h to reach steady state. The fluidized bed expanded with increasing the flow rate. Each experiment was terminated when the bed accumulated at the column's upper edge. At this critical flow rate bed escape commenced and it indicated transition to hydro-transportation regime, which was outside the scope of this research.

The experiments were performed over the whole range of inclination angles: from a horizontal to a vertical position of the pipe. Each experiment was conducted twice. First, the flow rate was increased from zero up to the maximal value associated with the bed escape; then the experiment was repeated by decreasing the flow rate back to zero. The pressure drop, flow rate and fluidized bed height were recorded several times at each point in both directions and were found to be identical within the error limits, regardless of the direction of the experiment. Hence, in the results presented below, each data point represents at least 2–3 measurements at a specified physical condition.

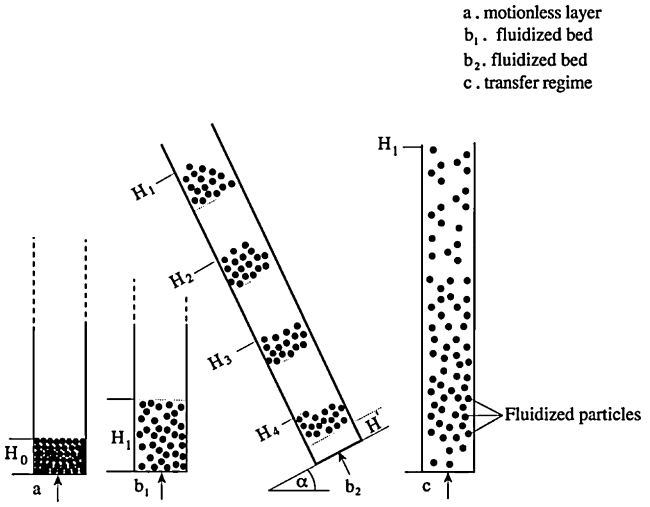

Fig. 2. Schematic descriptions of the development of the fluidized bed in vertical and inclined columns.

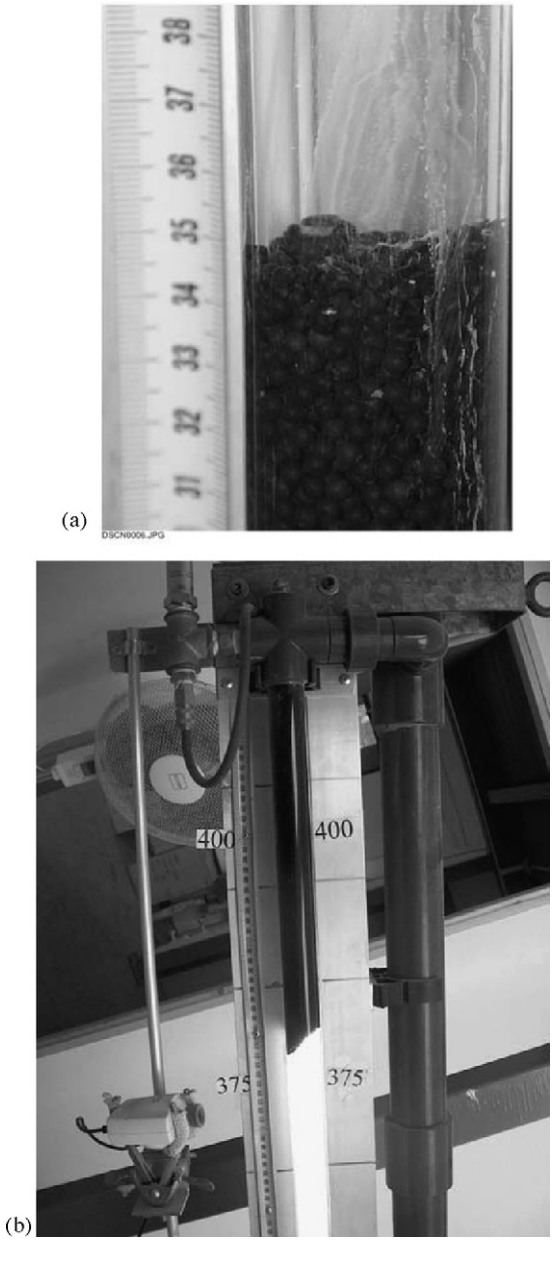

Fig. 3. Visualization of the fluidized bed at vertical and inclined columns: (a) flow of the fluidizing agent through the packed bed of particles, $\alpha = 90^\circ$, $Q = 0.4$ l/min; (b) escape of the fluidized bed in an inclined pipe, $\alpha = 60^\circ$, $Q = 7.3$ l/min. All particles accumulate at the column's top region.

3. Results and discussion

3.1. The dynamics of the fluidized bed—visual observations on the development of the fluidized bed

Visual observations suggest that the fluidization process and the bed escape are qualitatively different in horizontal and slightly upward inclined column ($\Delta\alpha_1 = 0$–20), inclined columns ($\Delta\alpha_2 = 20$–85) and in vertical or off vertical inclined columns ($\Delta\alpha_3 = 85$–90).

Fig. 2 shows schematically the fluidized bed in vertical and inclined columns. Figs. 3–5 show photographs of the bed structure in the different ranges of inclination angles. In Fig. 6, the bed height and structure are illustrated schematically for an initial bed of 35 cm height in columns with inclination angles of 0°, 20°, 40°, 70°, 80° and 90°, in the long pipe facility. In these graphs (Fig. 6) the vertical axis is the height along the pipe, while the horizontal axis represents the flow rate. In these experiments the flow rate was gradually increased from zero up to the escape flow rate associated with each inclination angle, and the bed was allowed to develop for a period of at least 1 h at each flow rate.

The present experimental study suggests that the whole process of development of the fluidized bed can be roughly divided into four modes related to the flow rate of the fluidizing agent. These are illustrated in Fig. 2 whereas the corresponding pressure drop is shown in Fig. 7a. The following categorization, originally suggested for vertical columns, is relevant also to off-vertical and inclined pipes.

- Mode I: flow of the fluidizing agent through the motionless packed bed of particles (Figs. 2a and 3a). In this region the pressure drop increases linearly with the flow rate (Fig. 7a, region AB)
- Mode II: initiation of fluidization and its development, or what is called *the first* fluidization region, where the value of the pressure drop does not depend on the fluidizing agent velocity (Figs. 2b_1 and b_2, 7a, region BC). This mode can be observed in vertical (90°) and near-vertical (e.g., 85°) inclination angles and is characterized by a decrease of the particle concentration with the bed height. The bed expands with the flow rate and the pressure drop is unchanged. This indicates that the decrease of the particles contribution to the pressure drop (due to the bed expansion) compensates the increase of the pressure drop with the water flow rate.
- Mode III: further increase of the flow rate leads the system to the *second* fluidization region (Fig. 2b_1 and b_2), where increasing the velocity of the fluidizing medium is accompanied by an increased pressure drop (see Fig. 7a, region CD). Some investigators [3] interpreted these phenomena as a sort of deviation from the theory. Particle motion in recirculation

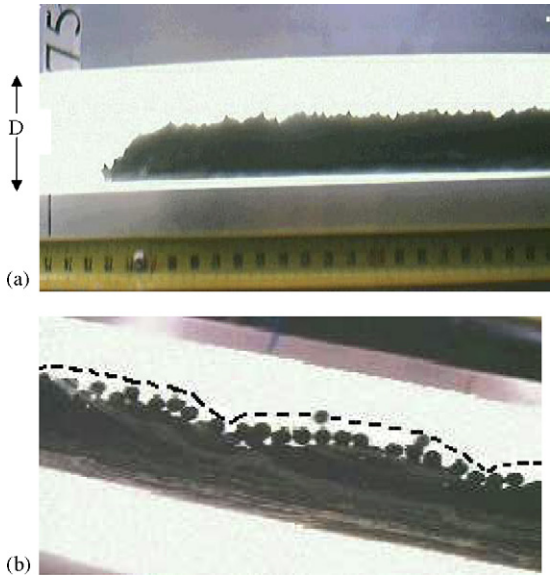

Fig. 4. Visualization of the fluidized bed at horizontal and near horizontal pipes: (a) $\alpha = 0^\circ$, $Q = 3$ l/min; (b) $\alpha = 20^\circ$, $Q = 5.5$ l/min.

cells could be observed with cell dimension between 10 and 20 cm. In *the first* fluidization region (Mode II) the cell dimension was between 5 and 10 cm. However, visual observations suggest that in Mode III the expanding bed reaches the column edge; redistribution of the particle concentration profile in the fluidized bed takes place whereby the concentration of particles increases downstream, resulting in a higher in situ fluid velocity and consequently an increased pressure loss. Mode III is terminated as the whole bed accumulates at the column top (see, for example, Fig. 3b for $\alpha = 60^\circ$). This flow rate is herein denoted as the critical flow rate for the escape of the bed and transition to particle hydro-transportation regime. This is the start of Mode IV, hydro-transportation, which is beyond the scope of this study.

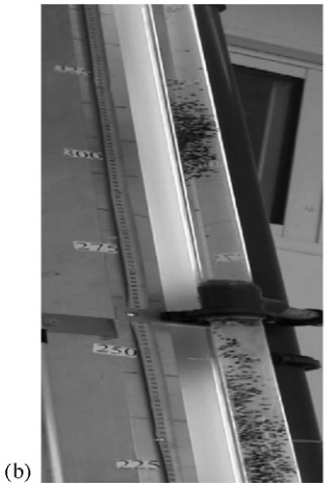

Fig. 5. Visualization of the fluidized bed at inclined pipes: (a) $\alpha = 40^\circ$, $Q = 4$ l/min; (b) $\alpha = 70^\circ$, $Q = 6.7$ l/min; In (b) groups of particles disintegrated from the main bed.

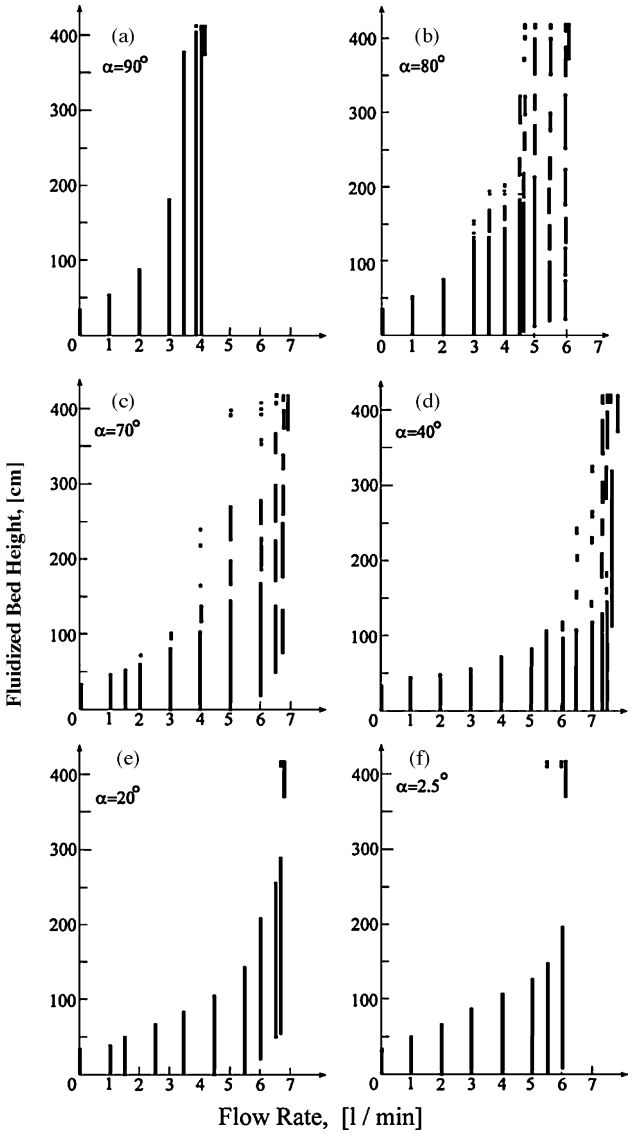

Fig. 6. A schematic illustration of the average location of groups of particles in the column at different flow rates and inclination angles of (a) 90°; (b) 80°; (c) 70°; (d) 40°; (e) 20°; (f) 2.5°. Each line segment represents the location of particles along the pipe. Vertical spaces between line segments represent water free of particles (see a schematic description in Fig. 2b$_2$ and the photograph of Fig. 5b).

In the extreme cases of nearly horizontal columns ($\Delta\alpha_1$), the process of momentum transfer is similar to that in a horizontal pipe [8]. Illustration of the flow pattern is shown in Fig. 4a. At

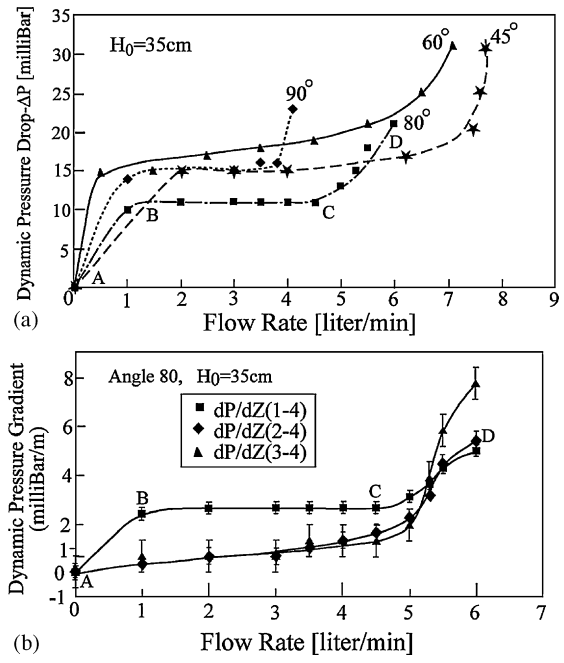

Fig. 7. (a) The dynamic pressure drop as a function of the flow rate. (b) Dynamic pressure gradient along different sections of the pipe.

the range $\Delta\alpha_1$, where the pipe is close to horizontal, particles are observed to be displaced upwards above a motionless layer of particles deposited along the lower pipe wall. As the fluid velocity is increased a motion of particles forming a wavy pattern (dunes) over a motionless bed is observed, as shown in Fig. 4b. The bed appears to creep upwards with its lower edge detached from the bottom of the pipe, forming a lower region of clear water which extends up to a distance of H' (Figs. 2b$_2$ and 6f). With a further increase of the fluid velocity the system approaches the stage where particles are detached from the top of the bed and reach the upper column edge. At this point a minute increase of the fluid flow rate results in accumulation of the entire bed at the upper edge of the tube.

The behavior is changed when the pipe inclination increases, $\alpha > 20°$. In inclined columns, the concentration of particles near the lower wall of the pipe is still greater than at the upper part, i.e., the density over the cross section decreases from the lower pipe wall (Fig. 5a). However, circulation of particles in the bed is observed with upward motion of the particles at the fluid/bed interface and downward motion of particles near the lower pipe wall.

With increasing the fluid flow rate the fluidized bed starts to be divided into groups of particles. A process of disintegration of the initial bed takes place whereby groups of particles separate from the bed, to form secondary beds (Figs. 5b and 6b, c, d). General observation suggests that the disintegration process continues and the number of fluidized beds increases with the flow rate. For example we consider in some detail the process at 80° (Fig. 6b). Up to a flow rate of 2 l/min, only one fluidized bed is observed, while at the flow rate of 3 l/min another bed starts above the lower one. The thickness of the secondary bed just formed is initially very small but it increases with the flow rate as observed at 3.5 l/min, where another bed (third bed) starts to form. The separation process is continued until the flow rate of 6 l/min, at which six fluidized beds can be observed. Each bed behaves like an isolated fluidized bed and is characterized by a flow structure and fluidized bed concentration similar to that of the continuous fluidized bed at nearly vertical columns. This phenomenon was not observed in a vertical pipe (see Fig. 6a).

The periodic structure of the secondary beds resembles a particle concentration wave with a characteristic wavelength, which depends on the column inclination and fluid flow rate. With increasing the fluid flow rate, this wave propagates upwards until it reaches the column's edge. At this point a minute increase of the fluid flow rate results in the escape of the whole bed towards the upper pipe edge as observed at the flow rate of 6.2 l/min (Fig. 6b). At this stage the experiment is terminated.

This sequence of events suggests that the bed escape is associated with the blockage of the concentration wave front. As such, the critical fluid velocity for the bed escape appears to be dependent on the column's length. However, the experiments carried out in the shorter column suggest a similar evolution process of the bed structure with a moderate effect of the column's length on the critical escape velocity for these two tested lengths (see Fig. 9c, below).

3.2. Quantitative results on the pressure drop, fluidized bed height and escape flow rate

3.2.1. The dynamic pressure drop

The dynamic pressure drop along the pipe as a function of the flow rate is shown in Fig. 7a, for $H_0 = 0.35$ m and four different inclination angles. This pressure drop is obtained by measuring the total pressure difference between the pipe inlet and outlet (P_1–P_4) and subtracting the hydrostatic pressure head measured without flow ($Q = 0$). This pressure drop thus includes the contribution of both the particles and the water flow. The contribution of the frictional water pressure drop (without particles) was estimated theoretically for the range of flow rates studied in these experiments; it was found to be smaller than 4% of the dynamic pressure drop due to both particles and water. Thus, the dynamic pressure drop presented in Fig. 7 is mostly due to the particles.

The results represent some important characteristics of the fluidized bed. For example, for $\alpha = 80°$, the range A–B represents the stage of flow through the packed bed of particles. The range B–C corresponds to the first stage of fluidization at which ΔP is nearly independent of the flow rate. As the inclination angle decreases, the range of the first fluidization stage becomes longer (in terms of the flow rate). This is observed in Fig. 7a where for 80° this stage (B–C) is longer than the corresponding stage for 90°. At 45° (and 30°, data not shown) the first fluidization stage is very long but at lower inclinations (e.g., 20°) it is difficult to identify this region.

Over the second fluidization region, the pressure loss increases with the flow rate, as shown in Fig. 7a (C–D). At this stage, the concentration of particles and the concentration of the fluidized bed increase downstream with height. The particles appear to make a large-scale motion with a variable orbit. This behavior is associated with the blockage of the concentration wave and conditions for the onset of bed escape are approached.

Fig. 7b shows the dynamic pressure gradient over different sections along the pipe for $\alpha = 80^\circ$ and $H_0 = 35$ cm. It is observed that during the different fluidization regions, the pressure drops along the different sections behave in a similar manner as the total pressure drop (P_1–P_4) along the pipe. During the first fluidization region (BC), the pressure gradient over Sections 2–4 is initially nearly constant (with increasing flow rate) but starts to increase as the flow rate increases above 3 l/min. This reflects the fact that more and more particles occupy the region of the pipe above the level of the sensor P_2 (1.05 m above the pipe inlet). A similar behavior is observed for the pressure gradient over section 3–4, but with a slower increase of the pressure gradient. At the second fluidization region (CD) the pressure gradient 3–4 reaches the highest value since at these high flow rates the particles tend to accumulate at the upper region of the pipe.

3.2.2. *The fluidized bed height*

In Fig. 8a and b, the variations of the dimensionless height of the fluidized bed with the water flow rate are shown. The fluidized bed height is defined as $\Delta H = H_1 - H_0$ where H_1 is the height of the upper edge of the (uppermost secondary) bed (Fig. 2a).

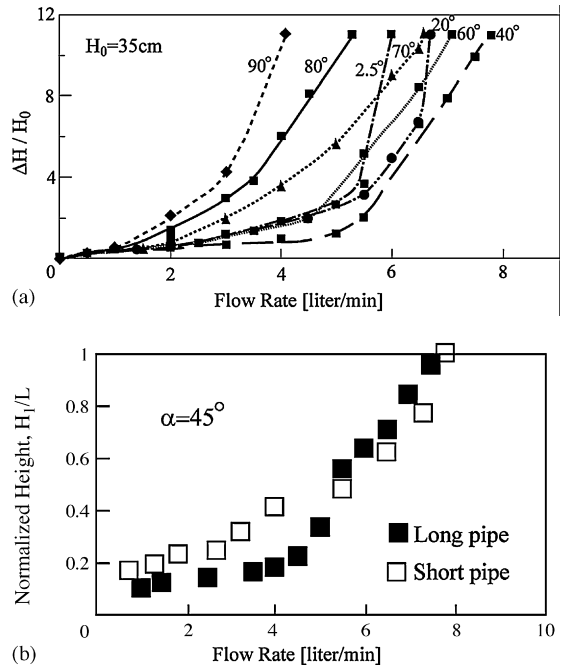

Fig. 8. (a) The height change of the fluidized bed normalized by the initial bed height, as a function of the flow rate, for seven different inclination angles. (b) A comparison between the fluidized bed expansion in the short and long columns.

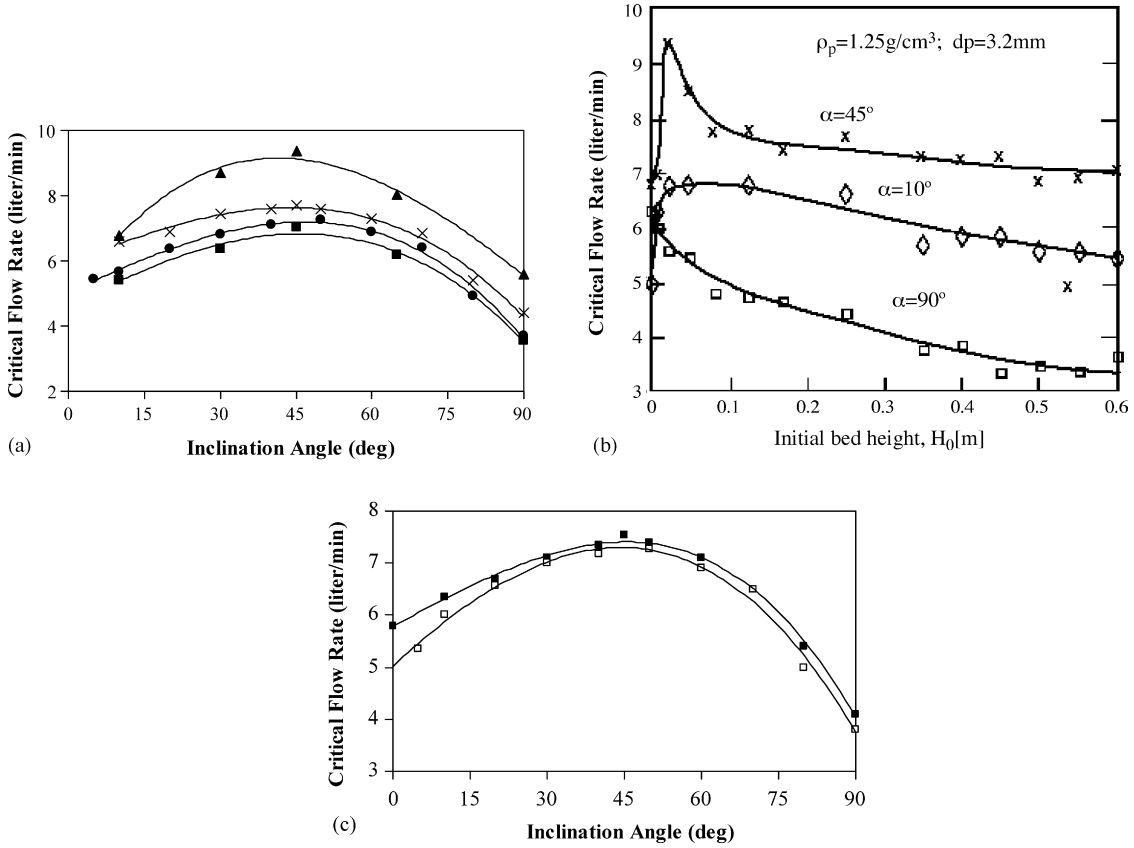

Fig. 9. (a) The critical flow rate for bed escape as a function of the inclination angle for different initial heights of the bed, H_0. Triangles: $H_0 = 0.025$ m ($Q_c = 10^{-5}\alpha^3 - 0.0035\alpha^2 + 0.229\alpha + 4.795$); $X - H_0 = 0.25$ m ($Q_c = -8 \times 10^{-6}\alpha^3 - 0.0002\alpha^2 + 0.0625\alpha + 5.925$); circles: $H_0 = 0.35$ m ($Q_c = -10^{-5}\alpha^3 - 5 \times 10^{-5}\alpha^2 + 0.0708\alpha + 5.04$); squares: $H_0 = 0.60$ m ($Q_c = -7 \times 10^{-6}\alpha^3 - 0.0004\alpha^2 + 0.083\alpha + 4.59$). (b) The effect of the initial bed height (particle concentration) on the critical flow rate for the bed escape. (c) The effect of the column's length on the critical flow rate for the bed escape, $H_0 = 0.35$ m. Full squares: long pipe; empty squares: short pipe.

In Fig. 8a, the bed height is normalized with respect to the initial bed height, H_0. The figure shows that the flow rate required for reaching a certain value of $\Delta H/H_0$ (before bed escape), increases as the inclination angle is reduced from 90° down to about 40°. As the inclination is reduced further below 40°, the required flow rate starts decreasing again. This trend in the extent of bed expansion is consistent with the trend observed later in the critical flow rate (see Fig. 9, below). Fig. 8b shows the height of the fluidized bed normalized with respect to the column's length, for both long and short pipes at $\alpha = 45°$. It is seen that at flow rates lower than the critical ones, the bed height is approximately independent on the column length as the normalized height at the short pipe is about twice that at the long pipe, in agreement with the ratio between the pipes lengths (=1.75, see Table 1). On the other hand, as the bed approaches the critical escape flow rate, the two beds have approximately the same normalized height, which means that the bed in the long pipe is about twice that in the shorter one. Thus, at this stage, where transition to hydro-transportation is approached, the bed's height is already constrained by the pipe length. Qualitatively similar results were obtained for other inclination angles.

3.2.3. The escape flow rate

The critical water velocity or flow rate for the onset of the bed escape is a key parameter for characterizing the range of operation of the bed. This critical flow rate is shown in Fig. 9a as a function of the pipe inclination angle for 4 out of the 6 initial heights of the particles, H_0. As H_0 increases from 0.025 to 0.6 m, the critical flow rate reduces for all inclinations, but the effect is most pronounced in inclination range $\alpha = 20$–$70°$. This result implies that a shorter initial bed can remain stable over a wider range of fluid flow rates. It is observed that at all values of H_0, the critical flow rate reaches a maximum value at inclination of about 45°. For example, at $H_0 = 0.35$ m and $\alpha = 45°$ the critical flow rate is nearly twice its value at 90°. Furthermore, when the inclination angle changed from about 45° to 0°, the critical flow rate for the bed escape decreased by about 30%. Notice that the critical flow rate for nearly horizontal pipes (∼5°) is always larger than that obtained for vertical pipes (90°).

The above variation of the critical flow rate with the inclination angle implies that the slippage between the water and particles is maximal at inclination of about 45°. In inclined pipes, the normal component of the gravitational force increases the "solid density" near the lower edge of the pipe. The axial gravitational component intensifies the slip velocity, between a particle and the continuous phase, in the axial direction. Both components enhance the slippage between the phases. The combined effect is maximal at some off-vertical inclination, which is observed to be at about 45° in this study.

Note that in this respect, it is interesting to refer to results obtained in oil/water (o/w) two-phase flows in upward inclined pipes (the oil phase is lighter). Mass balances show that the ratio between phase average velocities is given by

$$\frac{U_w}{U_o} = \frac{Q_w}{Q_o}\frac{\varepsilon_o}{1-\varepsilon_o}$$

where ε_o is the holdup, i.e., A_o/A. Therefore, the velocity ratio can be deduced from holdup measurements. Such measurements in oil-water (o/w) flows in upward inclined pipes [14] indicated that the largest deviations of the ratio of the average phase velocities (U_w/U_o) from the value of one (1) are obtained for pipe inclinations of about 45°. This implies that also in liquid–liquid systems, the slippage between the heavier and lighter phases is maximal at about 45°.

Fig. 9b shows the effect of the initial height of particles in the pipe, H_0, on the escape flow rate, at three different inclination angles, 10°, 45° and 90° (vertical pipe) and for $0 < H_0 \leq 0.6$ m. The limit case $H_0 \approx 0$ corresponds to experiments with few particles with a practically zero initial bed height, but finite escape flow rate. We first observe that for all inclinations, the initial particles height has a considerable effect on the escape flow rate. For inclined columns (10° and 45°) the escape flow rate initially increases with the bed height, up to about $H_0 = 0.025$ m, where the escape flow rate reaches a maximum value. For higher values of $H_0 > 0.025$ m, the escape flow rate generally decreases with H_0. The same result was obtained for inclinations of 30° and 65°, not shown in Fig. 9(b). In the case of a vertical pipe (90°) the behavior is different and the escape flow rate generally decreases with H_0, for the whole range of $0 < H_0 \leq 0.6$ m. In inclined tubes the lift force augmented by the lateral gravitational force directs the particles trajectory towards the tube wall where the local water velocity is lower. Consequently a circulation motion of the particles in the tube is induced and a larger water flow rate is required to transfer the particles away from the bed. For initial bed heights larger than approximately 0.4 m, the critical water flow rate seems to level off at a constant value. This constant value is smaller than the axial settling velocity calculated for a single particle carried by water moving at the average velocity. Measured settling velocity for a single particle in a vertical tube is 0.155 m/s. This is larger than the superficial velocity corresponding to bed escape conditions at 90° which, for $H_0 = 0.35$ m, is 0.12 m/s. However, the critical (escape) velocity of a thin bed (few particles) is about 0.2 m/s, which is significantly larger than the measured settling velocity (0.155 m/s). Also, in inclined tubes, the asymptotic value of the critical velocity is larger than the particle settling velocity.

A comparison between the escape flow rates in the long (LPF) and short (SPF) pipe facilities is shown in Fig. 9c for $H_0 = 0.35$ m. The figure shows that for all inclination angles, the escape flow rate in the long column is only very slightly larger than that in the short pipe (this can also be related to the small difference in the pipe diameters). Nevertheless, in both columns, the maximum escape flow rate is at inclination angle of about 45°.

Another type of experiments (conducted in the LPF only) was aimed at exploring the long-term behavior of the bed under a given flow rate. Thus, at each flow rate the system was allowed to operate over longer (0.5–1.5 h) and shorter (5–10 min) time periods. The results of the escape flow rate in Fig. 10 ($H_0 = 35$ cm) show that the escape flow rate is the same in both types of experiments for the inclination angle range of 20–60°. However, for other inclination angles, a small but consistent reduction of the critical flow rate is

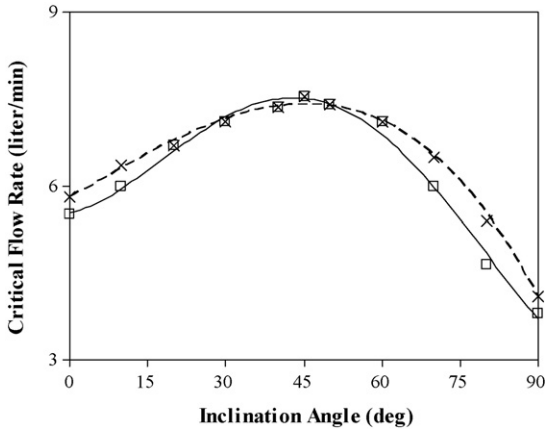

Fig. 10. The effect of the system's operation time on the dependence of the escape flow rate on the inclination angle for $H_0 = 35$ cm. X: short time; square: long time.

observed when the system is operating over longer time periods. Thus in these inclination angles, transient processes should be taken into consideration. In both cases, the maximum escape flow rate is obtained at inclination angle of about 45°.

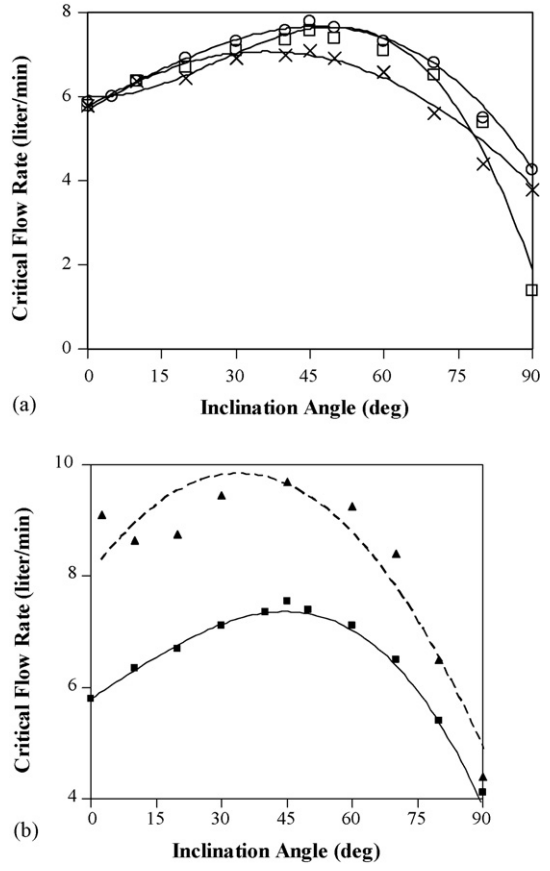

Fig. 11. The effect of (a) particle diameter and (b) particle density on the critical flow rate for the bed escape. Particle diameters in (a) are—X: 1.5 mm; square: 2.5 mm; circle: 3.2 mm. Particle density = 1.25 g/cm^3. Particle densities and diameters in (b) are—square symbols: $\rho_p = 1.25$ g/cm^3, $d_p = 1.5$ mm; triangle symbols: $\rho_p = 2.65$ g/cm^3, $d_p = 1.2$–1.4 mm; $H_0 = 0.35$ m.

3.2.4. The effect of particle density and diameter on the escape flow rate

The effects of particle diameter and density are presented in Fig. 11a and b respectively. Fig. 11a presents the critical flow rate for the bed escape as a function of the inclination angle, for three types of particles with the same density but different diameters (denoted as d_p). First it is observed that for all diameters, the critical flow rate reaches a maximum value at inclination of about 45°. The figure shows that the critical flow rate generally increases with the particle diameter. This effect is most pronounced for inclination angles higher than 20°. For inclinations below 20°, the effect of the diameter on the escape flow rate is very small. This can be explained by the observation that in this range of inclination angles, particles are observed to be displaced upwards above a motionless layer of particles deposited along the lower pipe wall.

Fig. 11b presents the escape flow rate as a function of the column's inclination angle, for particles of almost the same diameter, but substantially different densities. Again we observe that the maximum flow rate is at an inclination angle of about 45°. The results show that the critical flow rate increases significantly with the density for all inclination angles. For the heavier particles, however, the critical flow rate decreases as the inclination is reduced from 45° to 20°, but for inclinations smaller than 20° the critical flow rate is increased. This is because at these small inclinations (nearly horizontal pipe) the flow cannot transport the heavy particles that rest on the lower side of the pipe. Thus, a larger flow rate is required to transfer these particles away from the bed.

4. Conclusions

An experimental study was carried out to investigate the structure and dynamics of a fluidized bed in inclined pipes. The parameters, which characterize the fluidization process, change significantly with the pipe inclination angle. The following conclusions can be drawn from the experimental results:

- The critical flow rate for the bed escape attains a maximal value in columns inclined at about 45°. The critical flow rate increases with reducing the initial bed height and/or with increasing the particle diameter and density.
- In inclined columns, the fluidization process is characterized by disintegration of the initial bed into several secondary beds forming a pattern of a concentration wave. The experiments imply on a mild effect of the column's length on the critical flow rate.

As mentioned in the introduction, the results of this study may be important, for drilling inclined oil wells. During the drilling process, drilling mud is introduced into the well to transport the soil out. In this case flow rates larger than the critical one for bed escape are required in order to pump out the soil while drilling. On the other hand, when the oil is pumped, and pure oil is required, it is necessary to leave the soil particles as a fluidized bed, thus preventing the bed escape. Sub-critical flow rates should be applied at this stage. Thus, knowledge of the

critical flow rate for bed escape under different inclination angles is of major practical use.

Acknowledgments

The authors thank Mr. S. Shargorotski for his technical assistance with the experimental apparatus. B.Y. was partially supported by the Israeli Ministry of Absorption.

References

[1] B. Yakubov, Effective technological processes in oil-gas extraction—mechanics of fluidized bed, Baku Azerneshr (1990) 160.
[2] Y. Tsuji, T. Kawaguchi, T. Tanaka, Discrete particle simulation of two-dimensional fluidized bed, Powder Technol. 77 (1993) 79–81.
[3] M. Leva, Fluidization, McGraw-Hill, New York, 1959.
[4] J.F. Davidson, D. Harrison, Fluidization, Academic Press, London, New York, 1985.
[5] L.G. Gibilaro, Fluidization Dynamics, Butterworth-Heinemann, 2001, p. 256.
[6] D.P. O'dea, V. Rudolph, Y.O. Chong, L.S. Leung, The effect of inclination on fluidized beds, Powder Technol. 63 (1990) 169–178.
[7] C. Hudson, C.L. Briens, A. Prakash, Effect of inclination on liquid–solid fluidized beds, Powder Technol. 89 (1996) 101–113.
[8] P. Doron, M. Simkhins, D. Barnea, Flow of Solid–Liquid Mixtures in Inclined Pipes, Department of Fluid Mech. and Heat Transfer, Tel-Aviv University, 1996, pp. 1–22.
[9] D. Ercolani, G. Giachetta, A. Pareschi, Experimental analysis of solid sediment behavior in sloping pipes for solid–liquid mixtures, J. Pipelines 6 (1987) 205–216.
[10] M. Sarkar, S.K. Gupta, M.K. Sarkar, An experimental investigation of the flow of solids from a fluidized bed through an inclined pipe, Powder Technol. 64 (1991) 221–231.
[11] K. Hutter, T. Scheiwiller, Mechanics of Granular Materials, Elsevier Science Publishers, 1983, p. 283.
[12] J.H. Masliyah, H. Nasr-El-Din, K. Nandakumar, Continuous separation of bidisperse suspensions in inclined channels, Int. J. Multiphase Flow 15 (5) (1989) 815–829.
[13] L.S. Leung, P.J. Jones, Flow of gas–solid mixtures in standpipes. A review, Powder Technol. 20 (1978) 145–160.
[14] J.G. Flores, 1997. Oil–water flow in vertical and deviated wells. PhD dissertation, The University of Tulsa, Tulsa, Oklahoma, USA.